

Medium-range structure motifs of complex iron oxides

HPSTAR
1408-2022Cite as: J. Appl. Phys. **131**, 070902 (2022); doi: [10.1063/5.0082503](https://doi.org/10.1063/5.0082503)

Submitted: 15 December 2021 · Accepted: 1 February 2022 ·

Published Online: 18 February 2022

Shengxuan Huang¹ and Qingyang Hu^{2,a)}

AFFILIATIONS

¹Key Laboratory of Orogenic Belts and Crustal Evolution, MOE, Peking University and School of Earth and Space Sciences, Peking University, Beijing 100871, People's Republic of China

²Center for High Pressure Science and Technology Advanced Research, Beijing 100094, People's Republic of China

^{a)}Author to whom correspondence should be addressed: qingyang.hu@hpstar.ac.cn

ABSTRACT

Natural occurring iron oxides, such as Fe₂O₃, Fe₃O₄, and FeO, are abundant on Earth's surface and feature many implications in our daily life since the Iron Age, the final epoch of the prehistory of humanity. The physics of iron oxides is at the frontier of physical research due to their complicated magnetic and electronic properties. What makes it even more intriguing is the introduction of pressure, which not only regulates the crystal structures and physical properties, but also creates new iron-oxide stoichiometry. Recent studies discovered several novel iron-oxygen compounds under various pressure-temperature conditions. Despite different Fe/O ratios, those iron oxides are built upon similar structural units including FeO₆ octahedra and trigonal prisms. Complex stoichiometry of pressurized iron oxides is built up by stacking layers of those FeO₆ units, and in the medium-range, they are organized by certain structural motifs. In this perspective, we go beyond conventional iron-oxygen binary compounds and reveal the general formation mechanism of complex iron oxide crystals under high-pressure conditions. The results will be helpful for summarizing literary works of iron oxides and exploring novel stoichiometry with optimal physical properties.

Published under an exclusive license by AIP Publishing. <https://doi.org/10.1063/5.0082503>

I. INTRODUCTION

The electronic structure and stoichiometry of iron oxides, in the traditional view of physics, is controlled by the valence state of iron. Except for the single-element iron and oxygen, iron is in either +2 or +3 and iron oxide is largely discovered as FeO, Fe₂O₃, and Fe₃O₄ (equivalent to FeO + Fe₂O₃ in composition) on the Earth's surface. The variation of iron valence states and the semiconducting nature of iron oxides have been applied in all aspects of sciences. For example, electron hopping between Fe³⁺ and Fe²⁺ is utilized as a resistance switch in electrical devices.¹ The transformation between Fe³⁺ and Fe²⁺ is the source of energy for anoxygenic phototrophic bacteria that also supplies life-essential compounds in the early Earth.² In addition, the oxygen fugacity of the Earth's interior is determined by the Fe³⁺-Fe²⁺-Fe⁰ buffers, which predominantly control the physical and chemical processes inside the Earth.³

While temperature is well-known to alter the physical properties and trigger phase transitions of iron oxides,⁴ pressure has recently been realized as an equivalently important thermodynamic variable that imposes similar effects. The pressure-induced high-

low-spin transition collapses the magnetic ordering of FeO⁵ and Fe₂O₃ (Ref. 6) and substantially changes their electronic structures. Iron oxides of FeO and Fe₃O₄ feature large onsite Coulomb repulsion and small charge-transfer energy, which are both controlled by pressure.⁷ Recent experiments and theoretical predictions also suggest that pressure plays a key role in reshaping the stability fields of iron oxides through the modulation of enthalpy and that ambient stable FeO, Fe₃O₄, and Fe₂O₃ will react to form novel stoichiometry. Those compounds are only stable under high-pressure conditions and feature unique physical properties. In the Secs. II-V, we will review literary works and attempt to generalize the structural formulism of complex iron-oxides under high pressures.

II. MIXED-VALENCE “*m*FeO · *n*Fe₂O₃” IRON OXIDES

Several iron oxides with unconventional stoichiometry, such as Fe₄O₅,⁸ Fe₅O₆,⁹ Fe₅O₇,¹⁰ Fe₇O₉,¹¹ and more complicated compounds were predicted by theory,¹² some of which have been successfully synthesized at pressures of 10 ~ 80 GPa and annealed from high temperatures. These novel compounds hold Fe/O atomic

ratios of 0.667–1.000, which can be considered as the assemblage of “ $m\text{FeO} \cdot n\text{Fe}_2\text{O}_3$ ” (Table I).^{8–11,13–16} Considering the arrangements of Fe–O polyhedron building blocks and the oxidation states of iron, these compounds have similar topological crystal structures. The alternate stacking of FeO_6 octahedra and FeO_6 trigonal prisms along the a – b plane sets the m/n ratio and those propagating along the c axis determine the m value. For instance, the post-spinel phase of Fe_3O_4 , and novel Fe_4O_5 and Fe_5O_6 are categorized as $m\text{FeO} \cdot n\text{Fe}_2\text{O}_3$ ($m = 1, 2, 3$) or $\text{Fe}_t^{2+}\text{Fe}_{3+t}^{3+}\text{O}_{3+t}$ ($t = 1, 2, 3$) with the same space group of $Cmcm$. The monoclinic $C2/m$ $m\text{FeO} \cdot 2\text{Fe}_2\text{O}_3$ ($m = 1, 3, 5$) [or $\text{Fe}_t^{2+}\text{Fe}_4^{3+}\text{O}_{6+t}$ ($t = 1, 3, 5$)] class includes Fe_5O_7 , Fe_7O_9 , and Fe_9O_{11} . Their crystallographic information and synthesis conditions can be found in Table I.^{8–11,13–16}

Those novel iron oxides are different in the Fe/O ratio but have exhibited similar crystallographic signatures. The lengths of the b axis in these compounds correspond to one layer of FeO_6 polyhedra, which is in between 2 and 3 Å varied from 10 to 100 GPa.^{10,11} And the increase of m or n value does not affect the length of the b axis in both categories. The addition of FeO_6 octahedra or FeO_6 trigonal prisms to an $m\text{FeO} \cdot n\text{Fe}_2\text{O}_3$ compound will be stabilized by pressure and consequently, increase its a/b and c/b ratios. In addition, a larger n value is likely to lower the symmetry of $m\text{FeO} \cdot n\text{Fe}_2\text{O}_3$ compounds, which is caused by the distortion of connected FeO_6 octahedron and FeO_6 trigonal prism blocks. It is possible that incorporating more FeO_6 polyhedra into the crystal framework will lower its structural symmetry to the triclinic group and eventually break its long-range order, which may be a precursor of an iron oxide glass.

III. THE STRUCTURAL MOTIFS IN BUILD IRON OXIDE

The structure of iron oxides in the formula $m\text{FeO} \cdot n\text{Fe}_2\text{O}_3$ can be generalized by stacking layers of FeO_6 polyhedra and extended the layer in a specific pattern along the two-dimensional space. While the short-range of Fe–O polyhedra can be readily identified as FeO_6 octahedra and trigonal prism, the medium range which defines the way of how FeO_6 polyhedra are connected and arranged to fill three-dimensional (3D) space, controls the geometry of those high-pressure complex iron oxides. Here, we take one type of the arrangements of

FeO_6 polyhedron as an example (Fig. 1).^{8–10,16} For the class of $Cmcm$ -type $m\text{FeO} \cdot n\text{Fe}_2\text{O}_3$, the a – c plane is composed of isolated FeO_6 trigonal prisms (red square) and the polyhedral chains (black squares in Fig. 1) include one FeO_6 trigonal prism, followed by FeO_6 octahedra. The length of the chain determines the Fe/O ratio, with two, three, and four FeO_6 octahedra for Fe_3O_4 , Fe_4O_5 , and Fe_5O_6 , respectively. Consequently, adding one more FeO_6 octahedra to the polyhedral chain is equivalent to adding a “FeO” unit to $m\text{FeO} \cdot n\text{Fe}_2\text{O}_3$ compounds.^{8,9} On the other hand, the addition of “ Fe_2O_3 ” units to the $\text{FeO} \cdot \text{Fe}_2\text{O}_3$ proto-framework does not alter the structural motif of the polyhedral chain, but it increases the number of isolated FeO_6 trigonal prisms. For instance, this number of trigonal prisms in the a – c plane increases from one in Fe_3O_4 to three in Fe_7O_{10} , corresponding to build-up “ Fe_2O_3 ” motifs. If both arrangements in the a – c plane can be achieved in an $m\text{FeO} \cdot n\text{Fe}_2\text{O}_3$ compound, we anticipate that a very large a – c plane will be formulated. At the same time, the b axis remains the same. In this case, mixed-valence iron oxides can possibly form a macromolecule ionic compound with predictable arrangements of medium-range structures. The synthesis of hexagonal $\text{Fe}_{25}\text{O}_{32}$ with large lattice parameters ($a = 2.6289$ Å, $c = 13.4275$ Å) from the dissociation of Fe_3O_4 at ~ 80 GPa and ~ 3000 K is an outstanding example of forming large size iron oxide molecules at extreme conditions.¹⁰

Provided that the arrangements of FeO_6 octahedra and trigonal prisms of $m\text{FeO} \cdot n\text{Fe}_2\text{O}_3$ compounds can vary under different synthesis conditions, there might be much more undiscovered complex iron oxides at high pressure–temperature conditions. The upper limit of the coupled m and n values of $m\text{FeO} \cdot n\text{Fe}_2\text{O}_3$ compounds remains unclear. The $m\text{FeO} \cdot n\text{Fe}_2\text{O}_3$ compounds are usually synthesized at high pressure–temperature conditions through the reduction of Fe_2O_3 or Fe_3O_4 by iron metal or high-temperature annealing. This established approach is readily to control the bulk chemical boundaries of the product, but unable to predict the exact stoichiometry and most of the time, multiple iron-oxides derived from the starting compositions will co-exist. In order to obtain a single-phase of above-mentioned iron-oxide, it is necessary to find an optimized transition pathway at certain pressure–temperature conditions.¹⁷ As illustrated above, these $m\text{FeO} \cdot n\text{Fe}_2\text{O}_3$ compounds predominantly consist of FeO_6 octahedra and trigonal prisms. The pressure–temperature stability field of these compounds is, therefore, primarily affected by the stability of FeO_6 building blocks. The coordination number of iron should increase at higher pressures, which may destroy the current crystal framework of iron oxides. For instance, upon further compression, a FeO_6 octahedron can transform into a FeO_8 cube and a FeO_6 trigonal prism into a FeO_8 bicapped trigonal prism.¹⁸ In such a scenario, the medium-range structural motifs of $m\text{FeO} \cdot n\text{Fe}_2\text{O}_3$ compounds will be renovated. The structural and electronic properties of those materials may be predicted by the random structure searching algorithm and first-principles calculations.

IV. HIGH-PRESSURE PHYSICAL PROPERTIES OF COMPLEX IRON OXIDES

The sub-lattice spin states of iron cations play a key role in modulating magnetic and electronic properties of iron oxides. Cation iron can be in a high-spin (HS), intermediate-spin (IS), or low-spin (LS) state depending on the competition between Hund’s exchange term J and the crystal-field splitting energy Δ_{CF} .¹⁹ A

TABLE I. Novel mixed-valence iron oxides synthesized in the range of 10–80 GPa.^{8–11,13–16}

Chemical formula	Fe/O ratio	Space group	Synthesized conditions
FeO	1.000	$Fm\bar{3}m/R\bar{3}m$	$R\bar{3}m$: Room temperature, $>10 \sim 16$ GPa ¹³
Fe_5O_6	0.833	$Cmcm$	$10 \sim 20$ GPa, 2000 K ⁹
Fe_9O_{11}	0.818	$C2/m$	12 GPa, 1598 K ¹⁴
Fe_4O_5	0.800	$Cmcm$	$10 \sim 20$ GPa, 1500 \sim 2200 K ⁸
$\text{Fe}_{25}\text{O}_{32}$	0.781	$P\bar{6}2m$	80 GPa, 2950 K ¹⁰
Fe_7O_9	0.778	$C2/m$	$24 \sim 26$ GPa, 1873 \sim 1973 K ¹¹
$h\text{-Fe}_3\text{O}_4$	0.750	$Cmcm$	41 GPa, 1000 \sim 1200 K ¹⁵
Fe_5O_7	0.714	$C2/m$	71 GPa, 2700 \sim 3000 K ¹⁰
Fe_7O_{10}	0.700	$Cmcm$	64 GPa, 1800 \sim 2100 K ¹⁶
$\text{Fe}_{6,32}\text{O}_9$	0.702	$P6_3/m$	52 GPa, 1200 K ¹⁶
$\eta\text{-Fe}_2\text{O}_3$	0.667	$Cmcm$	55 GPa, 1500 K ¹⁰

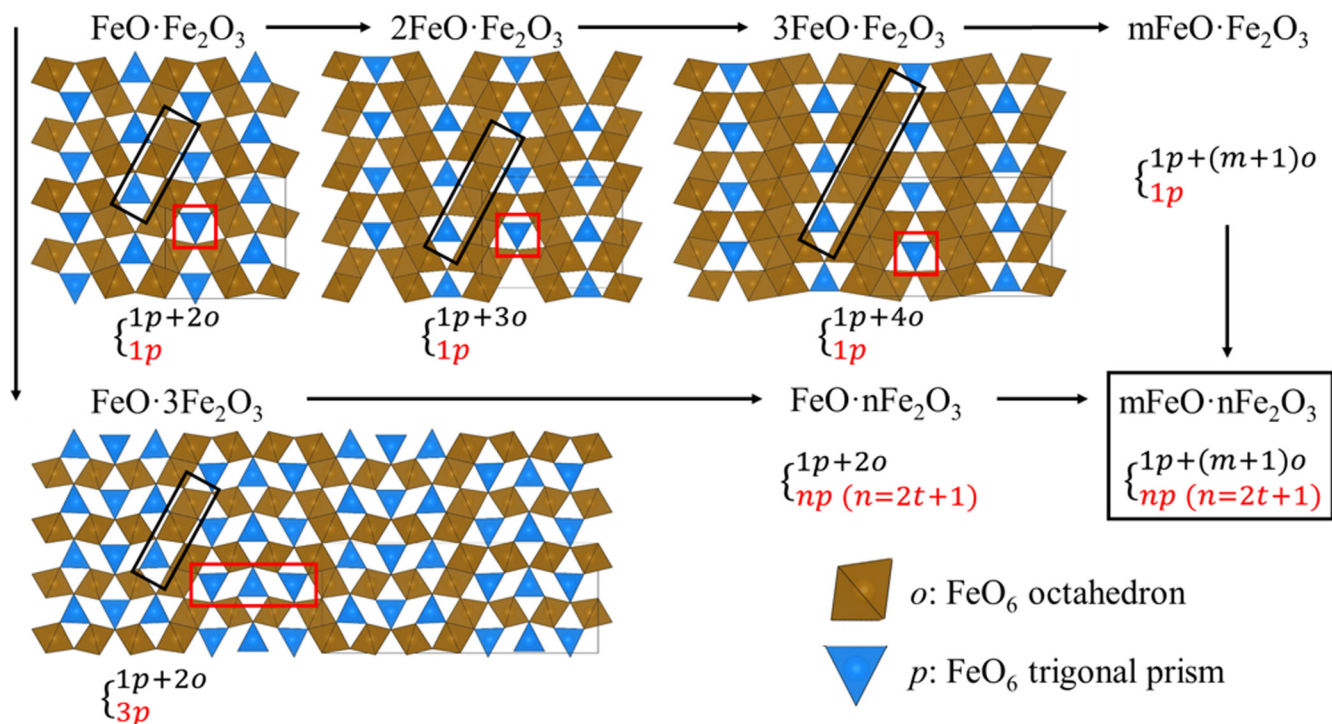


FIG. 1. Illustration of the arrangements of FeO_6 octahedra and trigonal prisms in the a - c plane of $Cmcm$ -type $m\text{FeO} \cdot n\text{Fe}_2\text{O}_3$ compounds. Black and red squares represent building units of an $m\text{FeO} \cdot n\text{Fe}_2\text{O}_3$ compound. Fe_3O_4 , Fe_4O_5 , Fe_5O_6 , and Fe_7O_{10} are written as $\text{FeO} \cdot \text{Fe}_2\text{O}_3$, $2\text{FeO} \cdot \text{Fe}_2\text{O}_3$, $3\text{FeO} \cdot \text{Fe}_2\text{O}_3$, and $\text{FeO} \cdot 3\text{Fe}_2\text{O}_3$, respectively. The crystal structures of selected compounds are constructed based on previous studies.^{5–10,16}

larger Δ_{CF} favors an LS or IS state in comparison with the HS state. At ambient conditions, the iron usually occupies the HS state in iron oxides. High pressure remarkably increases Δ_{CF} but slightly affects J , unpairing electron in the high energy level to stabilize them in the low energy level, which is the root cause of spin crossover (SCO). Pressure-induced SCO is sensitive to the medium-range structures, as was discussed in the previous section and may lead to the following distinct SCO behaviors: (i) site-selective SCO, (ii) reversal of SCO, and (iii) multi-stage SCO.

For ferric-only Fe_2O_3 , the Fe^{3+} cation of the octahedral site undergoes a HS–LS transition across the structural transformation at ~ 50 GPa, whereas that in the high-coordination site remains in the HS state.⁶ The Mössbauer spectrum shows that all Fe^{3+} in the θ -type Fe_2O_3 is in the LS state at ~ 70 GPa.¹⁰ However, heating this phase to high temperatures at ~ 70 GPa induces a θ - η structural transition as well as LS–HS reversal of half of Fe^{3+} .¹⁰ In terms of the mixed-valence iron oxide, Fe_3O_4 is predicted to suffer a four-stage SCO at different pressure points.²⁰ It is still under debate whether an IS state can be unambiguously derived in conventional Fe–O binary compounds. It is also an interesting physical question to differentiate or decouple the SCO of Fe^{2+} and Fe^{3+} in mixed-valence iron oxides. A recent first-principles simulation predicted those newly discovered mixed-valence iron oxides would exhibit similar multi-stage SCO upon compression.²¹ However, the site-selective SCO and its sequence in these materials remains

unanswered. The spin state and subsequent SCO in higher-coordination iron-oxide, for instance, CsCl-type FeO at pressures above 250 GPa and temperatures above 4000 K,²² are largely unknown but will be of fundamental interests to geophysicists.

The strong Coulomb repulsion between highly localized $3d$ electrons of iron cations opens up the bandgap of iron oxides, such as FeO and Fe_2O_3 , which are termed as the “Mott insulator.” It is also shown that pressure imposes profound effects in tuning the electronic structure near the Fermi level of iron oxides. Recent experiments support that the insulator–metal transition under high pressures is accompanied by the SCO.^{5,6} Pressure-induced SCO can cause a site-dependent collapse of local magnetic moments of iron. The magnetic collapse further leads to the delocalization of its $3d$ electrons at the selected site, which triggers the aforementioned electronic transition.

In mixed-valence iron oxides like magnetite, Fe^{2+} and Fe^{3+} randomly distribute in the octahedral site in inverse-spinel-type Fe_3O_4 at ambient conditions. The charge transfer at this site causes Fe_3O_4 to be a half-metal instead of an insulator. Fe_3O_4 undergoes a Verwey metal–insulator transition upon cooling to 125 K, driven by a charge ordering over linear three-Fe-site units.^{4,23} Similar phenomena were also detected in Fe_4O_5 and Fe_5O_6 ,^{24,25} and the charge-ordering temperature (T_{CO}) seems to be related to the Fe–Fe distance in their iron chains. Here, applying pressure will increase T_{CO} of those mixed-valence iron oxides by shortening the

Fe–Fe distance and promote the redistribution of $3d$ electrons at different sites. The modified electronic structure will lead to the transition to a new charge-ordering state, which is hindered at ambient conditions. As mentioned above, the SCO can delocalize the strongly correlated $3d$ electrons and destroy the charge-ordering state. Although pressure could promote electron hopping between Fe^{2+} and Fe^{3+} in mixed-valence iron oxides, thus far there is no clear evidence that pressure could oxidize or reduce a single iron cation. We regard in an $m\text{FeO} \cdot n\text{Fe}_2\text{O}_3$ compound the oxidation state of oxygen is -2 .

From the crystal chemistry point of view, macromolecule ionic mixed-valence iron oxides are comparable to the smaller ones, such as Fe_3O_4 and Fe_4O_5 , because these compounds share similar Fe–O building blocks. By contrast, their physical properties may be qualitatively different from those of small molecule oxides. For instance, the dimeric and trimeric orderings within iron ions are able to form in small molecule oxides, whereas macromolecule ionic compounds could exhibit polymeric ordering in the iron chain in the a – c plane. Under a certain arrangement of FeO_6 polyhedra, it is possible to form an inter-connected hexagonal charge-ordering ring in mixed-valence iron oxides like iron-based superconductors. Furthermore, the distinct arrangement of spins via the a – c plane from that along the b axis may contribute to a novel magnetic-ordering state under strong magnetic fields. Despite a macromolecule ionic compound and a small molecule iron oxide can have similar $\text{Fe}^{2+}/\text{Fe}^{3+}$ ratios, their cation distributions and consequently the magnetic-orderings depend on the way of how FeO_6 polyhedra structural motifs are connected and arranged.

On the basis of previous experimental and theoretical studies, we summarize that pressure increases the coordination number of iron and facilitates various arrangements of Fe–O polyhedra structural motifs, which governs their magnetic ordering and induces spin crossover of iron. These will further complicate the charge distribution and modify charge density across the Fermi level of these compounds. In this regard, pressure appears to be the fundamental factor controlling the physical properties of mixed-valence iron oxides. The phase diagram of each mixed-valence iron oxide as a function of pressure and the relative stability field across different compositions have not been fully understood by physicists. Understanding the relationship of these phenomena at high pressure–temperature conditions will also help to optimize their properties of “ $m\text{FeO} \cdot n\text{Fe}_2\text{O}_3$ ” iron oxides for industrial applications, such as spintronic devices, switches, and giant magnetoresistance materials.^{26,27}

V. BEYOND THE BOX OF FeO – Fe_2O_3

Besides conventional $m\text{FeO} \cdot n\text{Fe}_2\text{O}_3$, first-principles-based structure-searching algorithm investigations have demonstrated that iron oxides with more oxygen than Fe_2O_3 or more iron than FeO can stably exist under extreme conditions. Thus far, two oxygen-rich iron oxides have been experimentally determined (Fig. 2).^{28,29} (i) FeO_2 , adopting to the pyrite-type structure, was first synthesized by oxidization of Fe_2O_3 or decomposition of FeOOH above ~ 80 GPa under high temperatures.²⁸ (ii) The channel-structured $\text{Fe}_2\text{O}_{3+\delta}$ ($0 < \delta < 1$) phase was found to form in the $\text{Fe}_2\text{O}_3 + \text{H}_2\text{O}$ system at pressures of $40 \sim 90$ GPa and

temperatures above 1500 K.²⁹ Although the exact oxidation state of iron in pyrite-type FeO_2 is still under debate (Fe^{2+} or Fe^{3+}), all existing theoretical and experimental results suggest that its oxidation state is less than ferryl +4, which was found in CaFeO_3 .^{30,31} Those preliminary results on electronic structures indicate that the oxidation state of oxygen in two phases deviates from -2 . Note that once oxygen-rich iron oxides form, the oxidation state of iron or oxygen in a given crystal structure is not altered with increasing pressure in previous studies.^{28–31} And at extreme pressures, the structure type becomes a controlling factor of valences states.³² It remains unknown whether pressure could directly regulate the oxidation states of iron or oxygen at megabar pressures.

High pressure tends to stabilize an oxygen-rich iron oxide by shortening the distance between oxygen anions to form oxygen dimers, trimers, or even polymers, instead of promoting the charge transfer between iron and oxygen. This is consistent with the fact that oxygen-rich iron oxides can only be synthesized at high pressure–temperature conditions. Following this remark, we further hypothesize that it is possible to squeeze more oxygen into an iron oxide under high pressures, e.g., in the interiors of giant gas planets. The oxygen-rich iron oxides containing oxygen polymers may potentially exhibit superconductivity at sufficient pressures, similar to dense metallic oxygen.³³ A recent theoretical study highlights the role of magnetic coupling of $3d$ electrons in controlling the formation of O–O bonding in pyrite-type transition metal compounds.³⁴ In light of this work, the pyrite-type CoO_2 peroxide is predicted to be stable above ~ 40 GPa, much lower than that for FeO_2 . Superoxides may be ubiquitous for $3d$ transition metal under high pressures. The magnetic coupling is reduced in oxygen-rich iron oxides doping with cobalt, nickel, or copper. The doped oxygen-rich iron oxides may, therefore, be synthesized at much lower pressures than those for their pure counterparts.

The non-stoichiometric nature of $\text{Fe}_2\text{O}_{3+\delta}$ is attributed to a partial occupation of oxygen in the channel of the “ Fe_2O_3 framework.”²⁹ This unique channel structure may result in anisotropic electrical and thermal conductivities along its c axis vs a – b plane, which provides new insights into the electronic–magnetic decoupling in strongly correlated electron materials. The physical properties of the non-stoichiometric class of oxygen-rich iron oxides may be significantly different from those of the stoichiometric ones, which certainly requires further investigations. More interestingly, unlike FeO_2 , $\text{Fe}_2\text{O}_{3+\delta}$ was synthesized above 40 GPa and safely quenched to ambient conditions without destroying its original crystal structure. It remains elusive whether the oxygen in the channel is a key to stabilize this oxygen-rich phase, because stoichiometric Fe_2O_3 does not crystallize in the channel structure either at ambient conditions or at high pressure–temperature conditions.

Recent high pressure–temperature experiments have also revealed that the pyrite-type FeO_2 could incorporate a significant amount of hydrogen between its inter-polyhedral oxygen atoms to form FeO_2H_x solid solutions ($0 < x \leq 1$).³⁵ The hydrogen-bearing FeO_2 is stable above 75 GPa and was observed by chemical reactions between iron (or iron oxides) and water.^{36–38} Of particular interest is the solid-to-superionic transition of pyrite-type FeO_2H_x at elevated temperatures under high pressures, where hydrogen diffuses freely in the entire solid FeO_2 lattice.³⁹ This quantum

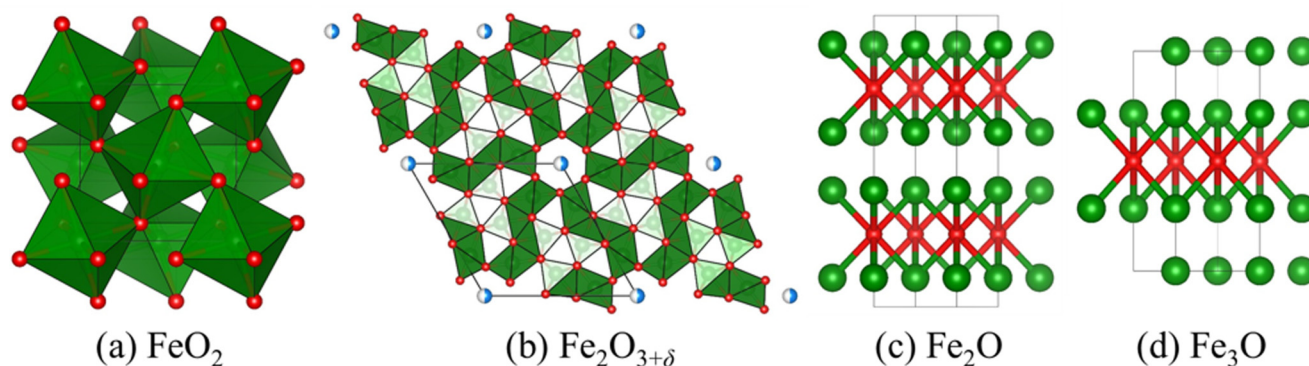


FIG. 2. Crystal structures of oxygen-rich (a) and (b) and iron-rich (c) and (d) iron oxides. The green and red spheres represent iron and oxygen atoms, respectively. The half-filled blue sphere in $\text{Fe}_2\text{O}_{3+\delta}$ represents the oxygen atom in the channel. The crystal structures of selected compounds are constructed based on previous studies.^{28,29}

behavior of hydrogen has far-reaching implications for the enigmatic electrical and thermal conductivities of the lower mantle. It thus is urgently needed to explore the superionic phases in other dense hydrous phases or even in nominal anhydrous phases.⁴⁰ Furthermore, theoretical simulations have predicted that FeO_2 has the capacity to react with inert elements (helium and xenon) at conditions of the lowermost mantle.^{41,42} Volatile-bearing FeO_2 exhibits a high density and extremely low seismic velocities in comparison with the normal mantle, which provides an alternative mechanism for the origin of ultra-low velocity zones located at the base of the mantle.^{36,41} These results indicate that the light and inert elements could be hosted in oxygen-rich iron oxides at the Earth's core-mantle boundary, and oxygen-rich iron oxides are, thus, possible candidate reservoirs of primordial volatiles. How the oxygen-rich phases affect the deep cycles and isotopic features of volatiles may set additional constraints on understanding the Earth's evolution and on assessing the habitability of planets.

On the other hand, the iron-rich iron oxides such as Fe_2O and Fe_3O ²⁸ were predicted to be stable at multi-megabar pressures because of the mismatch of iron and oxygen in atomic radius (Fig. 2). In their structures, oxygen can be considered to occupy the interstitial vacancy of close-packed iron and the structure is dominated by Fe-Fe metallic bonds. Therefore, these compounds are simply metallic. A previous theoretical study has shown that Fe_2O might be synthesized by direct combination of iron and FeO at approximately 300 GPa.⁴³ Although they are unlikely recovered to ambient pressure, the chemical bonding and charge transfer between iron and oxygen under extreme environments will make important constraints for the structure of Earth's core and exoplanetary interiors. For instance, iron-rich iron oxides affect the solubility of oxygen in liquid iron and change the melting behavior of the oxygen-bearing metallic melt. It is widely accepted that the Earth's liquid outer core (135–330 GPa) is primarily composed of iron and also contains several weight percent of oxygen. The stabilization of iron-rich iron oxides under extreme pressure may result in a heterogeneous distribution of oxygen at different depths of the outer core, and, therefore, considerably influence the geodynamics. In addition, the terrestrial super-Earth with a mass between 1 and 10 Earth masses have a silicate-dominant mantle and an iron-enriched core similar to our

planet. The pressure of the center of such planet may exceed 3000 GPa, where it may host iron-rich iron oxides as major compositions. The solidification of a super-Earth's core should be much more complex provided that various iron-rich iron oxides may form during the cooling of the core. Detailed investigations into the relative stability and physical properties of iron-rich iron oxides at extreme conditions are needed in order to better constrain the chemistry and physics of the Earth's and super-Earth's cores.

VI. CONCLUSION AND PERSPECTIVE

The state-of-the-art high pressure–temperature experiments combined with first-principles calculations have discovered various iron oxides with novel structures and stoichiometry. These achievements have contributed to the better understanding of a rather complex iron–oxygen system under extreme environments. Among them, of particular interest, is the family of mixed-valence $m\text{FeO} \cdot n\text{Fe}_2\text{O}_3$ compounds. These compounds share similar arrangements of FeO_6 octahedra and trigonal prisms which define their medium-range structures. In this respect, pressure may stabilize a novel class of complex iron oxides with large a - c planes. This layered-like structure may cause a long-range charge-ordering and a complicated magnetic–electronic coupling and be stress-sensitive. In addition, iron oxides composed of FeO_8 cubes and bicapped trigonal prisms may form at multi-megabar pressure ranges. It is still challenging to recover iron oxides synthesized under high pressures to ambient conditions due to their metastable nature. However, their crystal structure, bonding nature, and build-up structural motifs may guide us to discover novel iron oxide phases and will be useful to reveal the chemistry and physics of Earth's and planetary deep interiors.

ACKNOWLEDGMENTS

This study was financially supported by the National Science Foundation of China (NSFC) (Grant Nos. 42150101 and U1530402) and the CAEP Research Project (No. CX20210048). Q.H. is supported by the Tencent Xplorer Prize. S.H. acknowledges support from the Peking University Boya Postdoctoral Fellowship.

AUTHOR DECLARATIONS

Conflict of Interest

The authors have no conflicts to disclose.

DATA AVAILABILITY

The data that support the findings of this study are available from the corresponding author upon reasonable request.

REFERENCES

- ¹C. Yun, X. G. Chen, J. B. Fu, Y. X. Zhang, J. R. Sun, Y. F. Wang, Y. Zhang, S. Q. Liu, G. J. Lian, Y. C. Yang, C. S. Wang, and J. B. Yang, *J. Appl. Phys.* **115**, 17C306 (2014).
- ²F. Widdel, S. Schnell, S. Heising, A. Ehrenreich, B. Assmus, and B. Schink, *Nature* **362**, 834 (1993).
- ³A. Rohrbach, C. Ballhaus, U. Golla-Schindler, P. Ulmer, V. S. Kamenetsky, and D. V. Kuzmin, *Nature* **449**, 456 (2007).
- ⁴E. Verwey, *Nature* **144**, 327 (1939).
- ⁵K. Ohta, R. E. Cohen, K. Hirose, K. Haule, K. Shimizu, and Y. Ohishi, *Phys. Rev. Lett.* **108**, 026403 (2012).
- ⁶E. Greenberg, I. Leonov, S. Layek, Z. Konopkova, M. P. Pasternak, L. Dubrovinsky, R. Jeanloz, I. A. Abrikosov, and G. K. Rozenberg, *Phys. Rev. X* **8**, 031059 (2018).
- ⁷T. Muramatsu, L. V. Gasparov, H. Berger, R. J. Hemley, and V. V. Struzhkin, *J. Appl. Phys.* **119**, 135903 (2016).
- ⁸B. Lavina, P. Dera, E. Kim, Y. Meng, R. T. Downs, P. F. Weck, S. R. Sutton, and Y. Zhao, *Proc. Natl. Acad. Sci. U.S.A.* **108**, 17281 (2011).
- ⁹B. Lavina and Y. Meng, *Sci. Adv.* **1**, e1400260 (2015).
- ¹⁰E. Bykova, L. Dubrovinsky, N. Dubrovinskaia, M. Bykov, C. McCammon, S. V. Ovsyannikov, H.-P. Liermann, I. Kupenko, A. I. Chumakov, R. Rüffer, M. Hanfland, and V. Prakapenka, *Nat. Commun.* **7**, 10661 (2016).
- ¹¹R. Sinmyo, E. Bykova, S. V. Ovsyannikov, C. McCammon, I. Kupenko, L. Ismailova, and L. Dubrovinsky, *Sci. Rep.* **6**, 32852 (2016).
- ¹²G. L. Weerasinghe, C. J. Pickard, and R. J. Needs, *J. Phys. Condens. Matter* **27**, 455501 (2015).
- ¹³Y. Ding, Z. Cai, Q. Hu, H. Sheng, J. Chang, R. J. Hemley, and W. L. Mao, *Appl. Phys. Lett.* **100**, 041903 (2012).
- ¹⁴T. Ishii, L. Uenver-Thiele, A. B. Woodland, E. Alig, and T. B. Ballaran, *Am. Mineral.* **103**, 1873 (2018).
- ¹⁵L. S. Dubrovinsky, N. A. Dubrovinskaia, C. McCammon, G. K. Rozenberg, R. Ahuja, J. M. Osorio-Guillen, V. Dmitriev, H.-P. Weber, T. Le Bihan, and B. Johansson, *J. Phys. Condens. Matter* **15**, 7697 (2003).
- ¹⁶E. Koemets, T. Fedotenko, S. Khandarkhaeva, M. Bykov, E. Bykova, M. Thielmann, S. Chariton, G. Aprilis, I. Koemets, K. Glazyrin, H.-P. Liermann, M. Hanfland, E. Ohtani, N. Dubrovinskaia, C. McCammon, and L. Dubrovinsky, *Eur. J. Inorg. Chem.* **2021**, 3048 (2021).
- ¹⁷A. Ali, H. Zafar, M. Zia, I. ul Haq, A. R. Phull, J. S. Ali, and A. Hussain, *Nanotechnol. Sci. Appl.* **9**, 49 (2016).
- ¹⁸S. Xie, L. Wang, F. Liu, X. Li, L. Bai, V. B. Prakapenka, Z. Cai, H. Mao, S. Zhang, and H. Liu, *J. Phys. Chem. Lett.* **9**, 2388 (2018).
- ¹⁹D. Khomskii, *Transition Metal Compounds* (Cambridge University Press, Cambridge, UK, 2014), p. 37.
- ²⁰S. Ju, T. Y. Cai, H. S. Lu, and C. D. Gong, *J. Am. Chem. Soc.* **134**, 13780 (2012).
- ²¹Q. Y. Qin, A. Q. Yang, X. R. Tao, L. X. Yang, H. Y. Gou, and P. Zhang, *Chin. Phys. Lett.* **38**, 089101 (2021).
- ²²H. Ozawa, F. Takahashi, K. Hirose, Y. Ohishi, and N. Hirao, *Science* **334**, 792 (2011).
- ²³M. S. Senn, J. P. Wright, and J. P. Attfield, *Nature* **481**, 173 (2012).
- ²⁴S. V. Ovsyannikov, M. Bykov, E. Bykova, K. Glazyrin, R. S. Manna, A. A. Tsirlin, V. Cerantola, I. Kupenko, A. V. Kurnosov, I. Kantor, A. S. Pakhomova, I. Chuvashova, A. I. Chumakov, R. Rüffer, C. McCammon, and L. S. Dubrovinsky, *Nat. Commun.* **9**, 4142 (2018).
- ²⁵S. V. Ovsyannikov, M. Bykov, S. A. Medvedev, P. G. Naumov, A. Jesche, A. A. Tsirlin, E. Bykova, I. Chuvashova, A. E. Karkin, V. Dyadkin, D. Chernyshov, and L. S. Dubrovinsky, *Angew. Chem. Int. Ed.* **132**, 5681 (2020).
- ²⁶G. Maduraveeran, M. Sasidharan, and W. Jin, *Prog. Mater. Sci.* **106**, 100574 (2019).
- ²⁷T. Amrillah, C. A. C. Abdullah, D. P. Sari, Z. Mumtazah, F. P. Adila, and F. Astuti, *Cryst. Growth Des.* **21**, 7326 (2021).
- ²⁸Q. Hu, D. Y. Kim, W. Yang, L. Yang, Y. Meng, L. Zhang, and H. K. Mao, *Nature* **534**, 241 (2016).
- ²⁹J. Liu, C. Wang, C. Lv, X. Su, Y. Liu, R. Tang, J. Chen, Q. Hu, H. K. Mao, and W. L. Mao, *Natl. Sci. Rev.* **8**, nwa096 (2021).
- ³⁰J. Liu, Q. Hu, W. Bi, L. Yang, Y. Xiao, P. Chow, Y. Meng, V. B. Prakapenka, H. K. Mao, and W. L. Mao, *Nat. Commun.* **10**, 153 (2019).
- ³¹E. Koemets, I. Leonov, M. Bykov, E. Bykova, S. Chariton, G. Aprilis, T. Fedotenko, S. Clément, J. Rouquette, J. Haines, V. Cerantola, K. Glazyrin, C. McCammon, V. B. Prakapenka, M. Hanfland, H.-P. Liermann, V. Svitlyk, R. Torchio, A. D. Rosa, T. Irifune, A. V. Ponomareva, I. A. Abrikosov, N. Dubrovinskaia, and L. Dubrovinsky, *Phys. Rev. Lett.* **126**, 106001 (2021).
- ³²S. Zhu, J. Liu, Q. Hu, W. L. Mao, Y. Meng, D. Zhang, H. K. Mao, and Q. Zhu, *Inorg. Chem.* **58**, 5476 (2019).
- ³³K. Shimizu, K. Suhara, M. Ikumo, M. I. Eremets, and K. Amaya, *Nature* **393**, 767 (1998).
- ³⁴S. Huang, X. Wu, B. Hou, and S. Qin, *J. Phys. Chem. C* **124**, 10085 (2020).
- ³⁵Q. Hu, D. Y. Kim, J. Liu, Y. Meng, L. Yang, D. Zhang, W. L. Mao, and H.-K. Mao, *Proc. Natl. Acad. Sci. U.S.A.* **114**, 1498 (2017).
- ³⁶J. Liu, Q. Y. Hu, D. Young Kim, Z. Q. Wu, W. Z. Wang, Y. M. Xiao, P. Chow, Y. Meng, V. B. Prakapenka, H. K. Mao, and W. L. Mao, *Nature* **551**, 494 (2017).
- ³⁷H. Mao, Q. Hu, L. Yang, J. Liu, D. Y. Kim, Y. Meng, L. Zhang, V. B. Prakapenka, W. Yang, and W. L. Mao, *Natl. Sci. Rev.* **4**, 870 (2017).
- ³⁸L. Yuan, E. Ohtani, D. Ikuta, S. Kamada, J. Tsuchiya, H. Naohisa, Y. Ohishi, and A. Suzuki, *Geophys. Res. Lett.* **45**, 1330, <https://doi.org/10.1002/2017GL075720> (2018).
- ³⁹M. Hou, Y. He, B. G. Jang, S. Sun, Y. Zhuang, L. Deng, R. Tang, J. Chen, F. Ke, Y. Meng, V. B. Prakapenka, B. Chen, J. H. Shim, J. Liu, D. Y. Kim, Q. Hu, C. J. Pickard, R. J. Needs, and H. K. Mao, *Nat. Geosci.* **14**, 174 (2021).
- ⁴⁰Q. Hu and H. K. Mao, *Matter Radiat. Extrem.* **6**, 068101 (2021).
- ⁴¹J. Zhang, J. Lv, H. Li, X. Feng, C. Lu, S. A. T. Redfern, H. Liu, C. Chen, and Y. Ma, *Phys. Rev. Lett.* **121**, 255703 (2018).
- ⁴²F. Peng, X. Song, C. Liu, Q. Li, M. Miao, C. Chen, and Y. Ma, *Nat. Commun.* **11**, 5227 (2020).
- ⁴³S. Huang, X. Wu, and S. Qin, *Sci. Rep.* **8**, 236 (2018).